AFRL-RY-WP-TP-2011-1009

PULSE CHARACTERISTICS OF PASSIVELY MODE-LOCKED QUANTUM DOT LASERS (POSTPRINT)

Luke F. Lester, C.-Y. Lin, and Y. Li

University of New Mexico

D.J. Kane

Mesa Photonics

Nicholas G. Usechak and Vassilios Kovanis

Electro-optic Components Technology Branch
Aerospace Components Division

Y.-C. Xin

IBM Systems & Technology Group

JULY 2010

AIR FORCE RESEARCH LABORATORY
SENSORS DIRECTORATE
WRIGHT-PATTERSON AIR FORCE BASE, OH 45433-7320
AIR FORCE MATERIEL COMMAND
UNITED STATES AIR FORCE

REPORT DOCUMENTATION PAGE

Form Approved
OMB No. 0704-0188

1. REPORT DATE *(DD-MM-YY)*	2. REPORT TYPE	3. DATES COVERED *(From - To)*
July 2010	Conference Paper Postprint	15 September 2008 – 31 July 2010

4. TITLE AND SUBTITLE
PULSE CHARACTERISTICS OF PASSIVELY MODE-LOCKED QUANTUM DOT LASERS (POSTPRINT)

5a. CONTRACT NUMBER
In-house

5b. GRANT NUMBER

5c. PROGRAM ELEMENT NUMBER
61102F

6. AUTHOR(S)
Luke F. Lester, C.-Y. Lin, and Y. Li (University of New Mexico)
D.J. Kane (Mesa Photonics)
Nicholas G. Usechak and Vassilios Kovanis (AFRL/RYDP)
Y.-C. Xin (IBM Systems & Technology Group)

5d. PROJECT NUMBER
2305

5e. TASK NUMBER
DP

5f. WORK UNIT NUMBER
2305DP01

7. PERFORMING ORGANIZATION NAME(S) AND ADDRESS(ES)

University of New Mexico
Center for High Technology Materials
1313 Goddard SE
Albuquerque, NM 87106

Mesa Photonics
1570 Pacheco St. E-11
Santa Fe, NM 87505

Electro-optic Components Technology Branch (AFRL/RYDP)
Aerospace Components Division
Air Force Research Laboratory, Sensors Directorate
Wright-Patterson Air Force Base, OH 45433-7320
Air Force Materiel Command, United States Air Force

IBM Systems & Technology Group
Semiconductor Solutions
2070 Route 52
Hopewell Junction, NY 12533

8. PERFORMING ORGANIZATION REPORT NUMBER
AFRL-RY-WP-TP-2011-1009

9. SPONSORING/MONITORING AGENCY NAME(S) AND ADDRESS(ES)
Air Force Research Laboratory
Sensors Directorate
Wright-Patterson Air Force Base, OH 45433-7320
Air Force Materiel Command
United States Air Force

10. SPONSORING/MONITORING AGENCY ACRONYM(S)
AFRL/RYDP

11. SPONSORING/MONITORING AGENCY REPORT NUMBER(S)
AFRL-RY-WP-TP-2011-1009

12. DISTRIBUTION/AVAILABILITY STATEMENT
Approved for public release; distribution unlimited.

13. SUPPLEMENTARY NOTES
Conference paper published in the *Proceedings of SPIE Photonics West 2010*, Vol. 7616, 2010 (conference held in San Francisco, CA, January 23-28, 2010).

 This work is one of a number of manuscripts published in peer-reviewed journals as a result of in-house work on technical report AFRL-RY-WP-TR-2010-1195. This paper contains color and is available to the public.

14. ABSTRACT
Interest in quantum dot mode-locked lasers (QD MLLs) has grown in recent years since their first demonstration in 2001 as applications for optical time domain multiplexing, arbitrary waveform generation, and optical clocking are anticipated. Ultrafast pulses below 1 ps have been reported from QD MLLs using intensity autocorrelation techniques, but so far detailed characterization examining the pulse shape, duration, chirp, and degree of coherence spiking in these lasers has not been carried out. We describe the first direct frequency-resolved optical gating (FROG) measurements on a QD MLL operating at a repetition rate of 5 GHz.

15. SUBJECT TERMS
ultrafast, quantum dot, mode-locked lasers, pulse characterization

16. SECURITY CLASSIFICATION OF:			17. LIMITATION OF ABSTRACT:	18. NUMBER OF PAGES	19a. NAME OF RESPONSIBLE PERSON (Monitor)
a. REPORT	b. ABSTRACT	c. THIS PAGE			Nicholas G. Usechak
Unclassified	Unclassified	Unclassified	SAR	16	19b. TELEPHONE NUMBER *(Include Area Code)* N/A

Standard Form 298 (Rev. 8-98)
Prescribed by ANSI Std. Z39-18

Pulse characteristics of passively mode-locked quantum dot lasers

L. F. Lester[a], D. J. Kane[b], N. G. Usechak[c], C.-Y. Lin[a], Y. Li[a], Y.-C. Xin[d], and V. Kovanis[c]
[a]Center for High Technology Materials, University of New Mexico,
1313 Goddard SE, Albuquerque, NM 87106 USA
[b]Mesa Photonics, 1570 Pacheco St. E-11, Santa Fe, NM 87505 USA
[c]Air Force Research Laboratory, 2241Avionics Circle, Wright-Patterson AFB, OH 45433 USA
[d]IBM Systems &Technology Group, Semiconductor Solutions
2070 Route 52 Hopewell Junction, NY 12533 USA

ABSTRACT

Interest in quantum dot mode-locked lasers (QD MLLs) has grown in recent years since their first demonstration in 2001 as applications for optical time domain multiplexing, arbitrary waveform generation, and optical clocking are anticipated. Ultrafast pulses below 1 ps have been reported from QD MLLs using intensity autocorrelation techniques, but so far detailed characterization examining the pulse shape, duration, chirp, and degree of coherence spiking in these lasers has not been carried out. We describe the first direct frequency-resolved optical gating (FROG) measurements on a QD MLL operating at a repetition rate of 5 GHz.

Keywords: ultrafast, quantum dot, mode-locked lasers, pulse characterization

1. INTRODUCTION

As the speed of microprocessors using electrical clock distribution increases, the limitations of copper-based metal interconnects become more apparent. With the silicon CMOS feature size shrinking from today's state-of-the-art of 32 nm, speed bottlenecks due to RC delays on the chip and increasing electrical power consumption are expected to become serious problems[i, ii]. There is renewed interest in semiconductor MLLs as sources for multi-gigahertz, ultra-short optical pulse generation. The compact size, low cost, low power consumption, and direct electrical pumping of semiconductor monolithic mode-locked lasers make them promising candidates for inter-chip/intra-chip clock distribution[iii, iv] as well as other applications including high bit-rate optical time division multiplexing[v-ix], high speed electro-optic sampling[x], and impulse response measurement of optical components. However, the compact diode laser pulse sources have generally not been able to match the pulse quality of the best mode-locked lasers[xi]. They suffer from longer pulse durations, impaired stability, asymmetric pulses, chirped spectra and compromised peak power. To improve the characteristics of semiconductor mode-locked lasers, detailed pulse analysis is required[xii].

Ultrafast pulses from QD MLLs have been reported as short as 393 fs using intensity autocorrelation techniques[xiii], but only fairly recently has detailed characterization examining the pulse shape, duration, chirp, and degree of coherence spiking in these lasers been conducted[xiv - xvii]. In this work direct frequency-resolved optical gating (FROG) measurements on a QD MLL operating at a repetition rate of 5 GHz with typically 5-10 ps pulses. Since commercially available FROG devices lack the sensitivity required to measure the output pulses from QDMLLs, we built a unique, ultra-sensitive second-harmonic-generation FROG system. Good pulse retrievals were obtained from an 8.2-mm cavity length QD MLL that has a 1.1-mm long saturable absorber at average powers up to about 5-10 mW. FROG traces at higher average powers contained coherence spikes. These features are well known in intensity autocorrelations and are usually caused by laser instabilities, which are always "coherent" at zero time delay, causing a large and fictitiously narrow peak to occur. Unlike intensity autocorrelation, however, FROG is not susceptible to confusing these coherence spikes with the actual pulse width of the laser. In addition, the data shows a clear pulse asymmetry corresponding to a fast rise and slow fall time. The mostly linear chirp in the pulses indicates that recompressing the output can produce sub-picosecond pulses.

Novel In-Plane Semiconductor Lasers IX, edited by Alexey A. Belyanin, Peter M. Smowton,
Proc. of SPIE Vol. 7616, 761607 · © 2010 SPIE · CCC code: 0277-786X/10/$18 · doi: 10.1117/12.843738

2. DEVICE DESIGN, FABRICATION AND TEST SETUP

2.1 Device structure

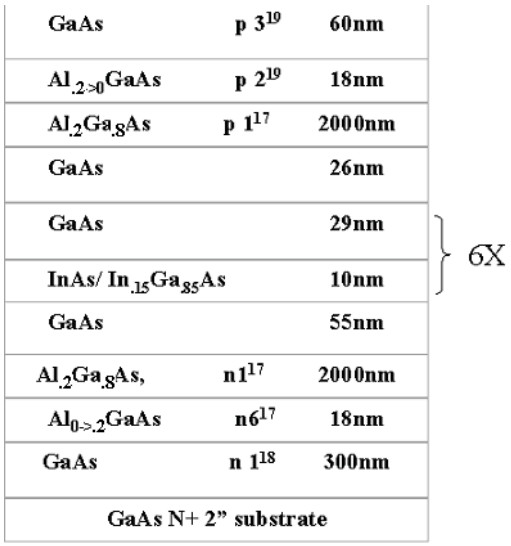

Fig. 1. The epitaxial structure of the 6-stack DWELL laser designed for high average power operation. An 8-stack version was also studied.

2.1 Multi-layer DWELL laser structure

The multi-layer DWELL laser structure is grown by molecular beam epitaxy (MBE) and consists of either 6 or 8 stacks of dots in the active region. The layers are composed of an n-type (10^{18} cm^{-3}) 300-nm-thick GaAs buffer, an n-type lower $Al_xGa_{1-x}As$ (x=0.2) cladding layer, a GaAs core waveguide, a p-type upper cladding layer, and a p-doped (3×10^{19} cm^{-3}) 60-nm-thick GaAs cap. The cladding layers are doped at 10^{17} cm^{-3} and are each 2-μm thick. In the center of the waveguide, 6 or 8 DWELL layers with 29 nm GaAs barriers were grown. QDs formed from about 2 monolayers of InAs are confined in the middle of a 10 nm thick $In_{0.15}Ga_{0.85}As$ QW in each layer. The QD's and QW were typically grown at 500 °C, as measured by an optical pyrometer. The QD's formed under these conditions have an areal density of about 3×10^{10} cm^{-2}, a base diameter <40nm, and are 7 nm high. Detailed descriptions of the DWELL growth technique can be found elsewhere[xviii,xix]. A schematic of the 6-stack DWELL version is shown in Fig. 1. A typical InAs DWELL laser structure has an internal loss of 1-2 cm^{-1} and a maximum net modal gain of 2-3 cm^{-1} per QD layer.

2.2 Device fabrication

The devices are typical 2-section ridge-waveguide lasers with a ridge width of 3.5 μm as shown in Figure 3. Devices were fabricated according to standard multi-section device processing[xx]. After the first lithography with the ridge-waveguide-mask, the sample was etched to form 3-μm wide, 1.8-μm deep ridges by inductively coupled plasma (ICP) etching in BCl_3. Then a BCB layer was applied for isolation between the p-type metal and the etched cladding layer. The two-section contact mask was used to make photoresist patterns for the p-type metal deposition and ion implantation. After depositing Ti/Pt/Au to form the p-metal contact, an isolation between the adjacent sections was provided by proton implantation, with an isolation resistance of >10 MΩ. After the substrate had been thinned and polished, a Au/Ge/Ni/Au n-metal contact was deposited on the backside of the n^+-GaAs substrate and annealed at 380°C for 1 minute to form the n-ohmic contact. A temperature greater than 380°C can crack the BCB. Another Ti/Au metal layer was deposited for n-side mounting, and then the sample was cleaved to form devices with a short absorber section and long gain section. In this work, the InAs DWELL MLL has a 1.2-mm absorber section and a 6.8-mm gain section. The cleaved facet near the absorber section was HR-coated (R≈95%) to create self-colliding pulse effects in the saturable absorber for pulse narrowing. The other facet was low reflection (LR)-coated (R≈15%). The devices were mounted on copper heatsinks, and for all the results presented in this paper, the measurements were performed at a controlled substrate temperature of 20°C if not specified.

2.3 The mode-locked laser measurement setup

The operational characteristics of MLLs that are measured include the repetition rate, the optical pulse width, the optical spectrum, the peak power, and the threshold current. The test setup includes two main blocks: an electrical-pumping block, and a signal-detection block, as shown in Fig. 2. A DC power source was used to apply a reverse bias on the absorber, and a laser diode controller was used to pump the gain section. An integrated optical head mounted on a 5-axis precision linear stage was used to collect the output emission of the mode-locked laser. The integrated optical head consists of a polarization-maintaining fiber (PMF) pigtail, a collection lens, and an isolator. The lens focuses the output light into the PMF through the isolator, which is used to avoid interference effects. The collected emission is fed into either the autocorrelator (Femtochrome FR-103XL) or the FROG system to measure the pulse width, and the optical spectrum analyzer to measure the optical spectra through fiber couplers. An RF spectrum analyzer (HP8563E) measures the repetition rate. The light-current (L-I) characteristics can be obtained if the optical head is replaced with an integrating sphere and photodetector.

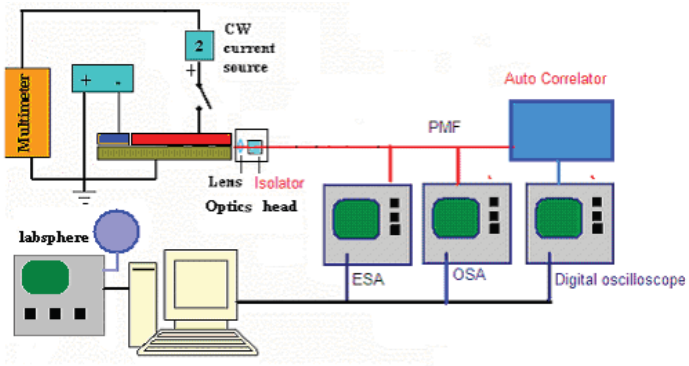

Fig. 2 Schematic diagram of the mode-locked laser measurement setup. The autocorrelator can be exchanged with the FROG system.

3. EXPERIMENTAL RESULTS

3.1 Basic Characteristics of the InAs DWELL MLLs

Some unique characteristics of QD lasers, such as the ultra-broad bandwidth, ultra-fast gain dynamics, easily saturated absorption, strong inversion, low alpha parameter and wide gain bandwidth, make them an ideal choice for semiconductor monolithic mode-locked lasers[xxi-xxiv]. Also the 1.24-μm emission wavelength, which is transparent to Si waveguides and detectable by SiGe photodetectors, makes the InAs QD mode-locked lasers suitable for Si-based optoelectronic integrated-circuits[xxv, xxvi].

To improve the peak and average powers, a low confinement factor waveguide with 20% AlGaAs cladding layers was designed in the InAs DWELL laser structure. Fig. 3 shows the pulse characteristics of the high power QD passive MLL module at 20°C as a function of the gain current and the absorber bias voltage. As the map shows, with an absorber bias of -5 V, the device produced 5 GHz optical pulses with a pulse width of less than 10 ps and a peak power of more than 550mW over a wide operating gain current range of 190 to 300 mA. There is small range of operation around a bias current of 270 mA and -5V on the absorber at which the peak power exceeds 1 W primarily because the pulse width abruptly narrows to less than 6 ps. This abrupt change in operational behavior could easily be an artifact of the autocorrelation measurement as will be described below. Fig. 4 displays the L-I curve and the optical spectrum under an absorber bias of -5V. The lasing occurred at the QD ground state (λ = 1240 nm) with a forward scan turn-on threshold of 160 mA, corresponding to a threshold current density of approximately 580 A/cm^2. Under a gain current of 270 mA and an absorber bias voltage of -5V, the device had a pulse width (Δt) of 5.7 ps as shown in Fig. 5 (b) according to the intensity autocorrelator. The electrical spectrum under the same bias conditions is shown in Fig. 5 (a), and the repetition rate f is 4.97 GHz. Therefore, the laser achieved a high peak power of 1.04 W, which is about 5 times higher than the peak power (≈200 mW) of QD MLLs with a high confinement factor waveguide[1].

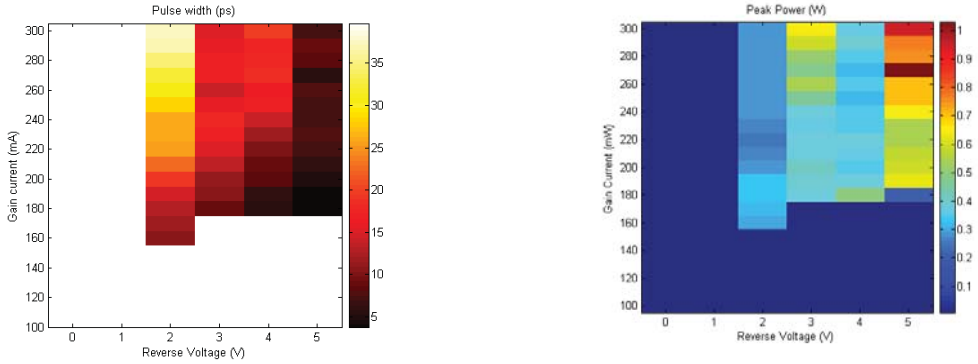

(a) (b)

Fig. 3 (a) Pulse width and (b) peak power mapping of the high-power QD passive MLL chip at 20°C with a reverse bias of 0-5 V and a gain current of 100-300 mA.

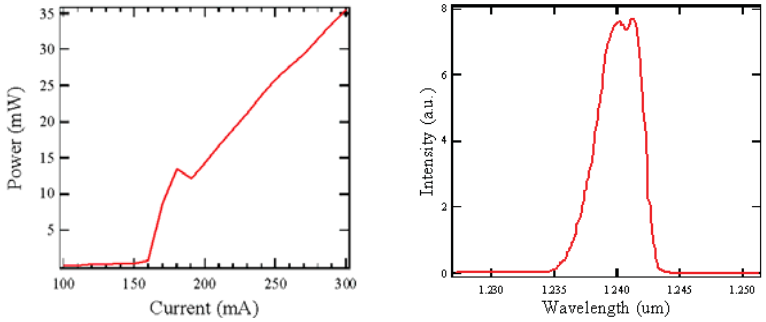

(a) (b)

Fig. 4 The CW L-I characteristics (a) and optical spectrum (b) of a 1240 nm QD passive MLL under absorber bias of -5 V. For the optical spectrum, the gain current is 270 mA.

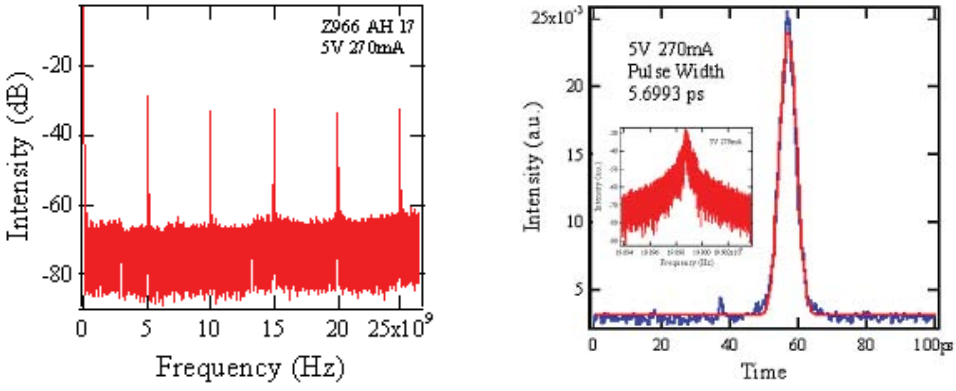

(a) (b)

Fig. 5 Mode-locked optical pulse characteristics of the high-power QD passive MLL module at 20°C with a reverse bias of 5V and a gain current of 270 mA. (a) Electrical spectrum showing a pulse repetition rate of 4.97 GHz. (b) The auto-correlation signal showing a pulse width of 5.7 ps. The inset figure shows the 4th harmonic electrical spectrum with a span of 10 MHz.

3.2 Frequency Resolved Optical Gating (FROG) setup and measurements

From a 5-GHz repetition rate device made from the 8-stack QD wafer, the optical output was collected with an optical head, which integrates a lens, an isolator and a short 1-m single-mode polarization maintaining (PM) fiber pigtail, and then coupled into the FROG system through the PM fiber. The FROG system includes a Femtochrome autocorrelator and a scanning monochromator as shown in the Fig. 6. The autocorrelator generates a background-free second harmonic generation (SHG) signal using a 1-mm thick $LiIO_3$ crystal. The SHG signal was guided out of the autocorrelator and coupled into the monochromator with a set of mirrors and lenses. The mirror inside the autocorrelator is removable, which permits intensity autocorrelation to be evaluated also. The SHG signal in the monochromator was spectrally gated and detected by a highly sensitive photomultiplier tube (PMT) that is placed at the output slit. The resulting electronic signal from the PMT was amplified with a low-noise current preamplifier and then recorded with a digital oscilloscope. By scanning the grating in the monochromator, SHG FROG traces were obtained with a computer.

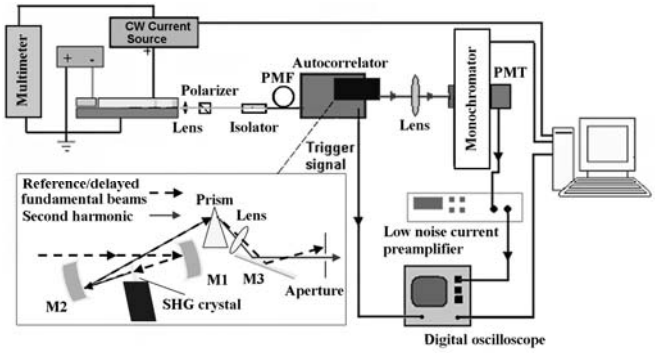

Fig. 6. Schematic diagram of the FROG system.

The pulse shapes of the 8-stack laser that were obtained from the autocorrelator are shown in the Fig. 7(a). The data show symmetric pulses of 7.2 – 9.0 ps at gain currents of 100mA – 110 mA and a reverse bias of -4 V, which correspond to 5.0 to 6.3 ps pulses assuming a Gaussian pulse shape. The optical spectrum of the MLL has a 4.3-nm FWHM. The time bandwidth products are about 4.2–about 12 times higher than their transform limit. Thus, with the intensity autocorrelation, we strongly suspect that the pulse is chirped, but it cannot be determined if this is due to dispersion or nonlinear effects.

FROG traces were obtained with different gain-currents and reverse biases. With a reverse bias of 3.5V-4V on the saturable absorber, good pulse retrievals were obtained at drive currents from 100-115 mA on the gain section of the QD MLL. Time domain pulse intensity profiles derived from the pulse retrievals for the FROG traces are shown in Fig. 7(b) at four different drive currents with an absorber bias of 4V. As the drive current increases, the length of the pulse stays constant until 115 mA drive. The lower drive current pulses are about 5-6 ps long while the 115 mA drive case is about 7-8 ps long. In all cases, a clear pulse asymmetry is observed. Since there is a time direction ambiguity in SHG FROG, the FROG measurements alone cannot determine which edge is the leading edge of the pulse. However, the differential absorption is much higher than the differential gain under these operating conditions. Hence the pulse should have a faster leading edge and a slower trailing edge.

Figure 8 shows the time domain phase of the retrieved pulses. They are relatively consistent from pulse to pulse. The data indicates that the pulses from the QD MLL are mainly linearly-chirped. These measurements indicate that operational conditions exist for the QD MLL for which the pulses are well-behaved and completely recompressible. The transform limited pulse width was determined to be about 600 fs by mathematically removing the spectral phase. While the bandwidth would support 300 fs pulses, spectral structure limits the ultimate pulse duration.

An SHG FROG trace from the monolithic mode-locked QD laser with a gain current of 105 mA and a reverse bias of 3.5V on the absorber is shown in Fig. 9(a). (The SHG FROG traces are symmetrized about t=0 before inversion.) The corresponding spectrogram of the pulse retrieved from this FROG trace is shown in Fig. 9(b).

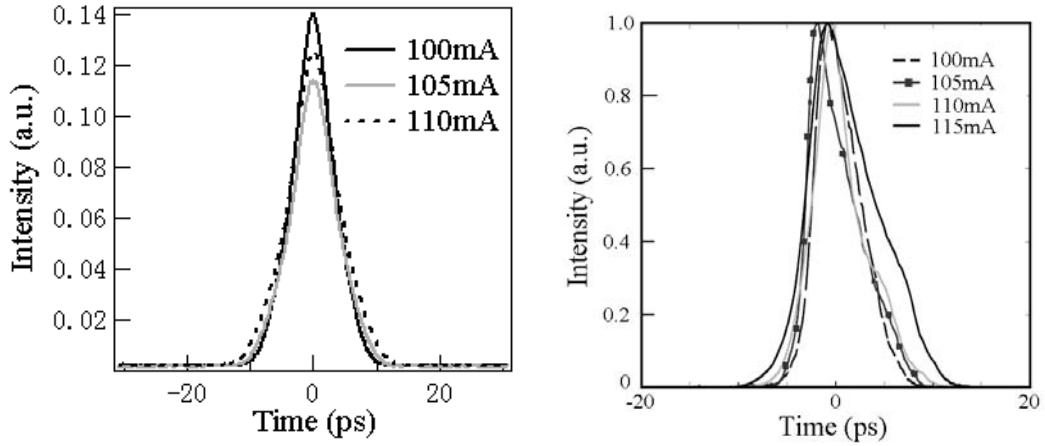

Fig. 7. The optical pulse shape of the device with different gain currents and a reverse bias of 4V applied on the 1-mm absorber of the 8-stack laser. (a) Pulse shapes obtained from intensity autocorrelations. (b) Time domain intensity profiles of the retrieved pulses from a series of FROG traces with an absorber bias of 4 V and drive currents from 100 mA to 115 mA.

FROG traces from higher drive currents (>120 mA) contained coherence spikes. Such features are well known in autocorrelation traces and are believed to be caused by laser instabilities. This idea is corroborated by the inability of the phase retrieval algorithm to converge for FROG traces containing coherence spikes. They occur because even random noise is always "coherent" at zero time delay, causing a large spike to occur at zero time delay, where the pulse replicas are overlapped exactly. In the case of true noise, the correlation function goes to zero at non-zero time delays. Non-random features have non-zero, but lower correlation values at non-zero time delay. If the pulse breakup is stable, then patterning of the FROG trace will appear, along with structure in the autocorrelation. Such patterning was not observed indicating that the pulse structure was not stable.

With the bias held at -3.5V, as the operating current is increased, the mode-locked pulse begins to break up. The pulse splits in two at a gain current of 130 mA as shown in the spectrogram in Fig. 10(b). This pulse break up is a typical failure mode of mode-locking in these laser systems. These results appear inconsistent with a completely inhomogeneously broadened system. "Pulse break-up" in this manner is consistent with the idea that quantum dots close in energy are coupled together. Therefore, from the pulse measurement data, it appears that there is homogeneous broadening in the QD system that has a FWHM of roughly 1-2 THz.

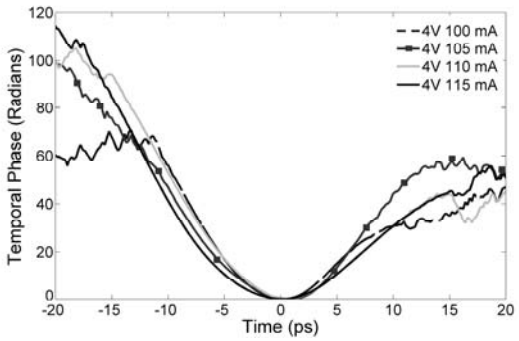

Fig. 8. Time domain phase of the retrieved pulses shown in Figure 7(b).

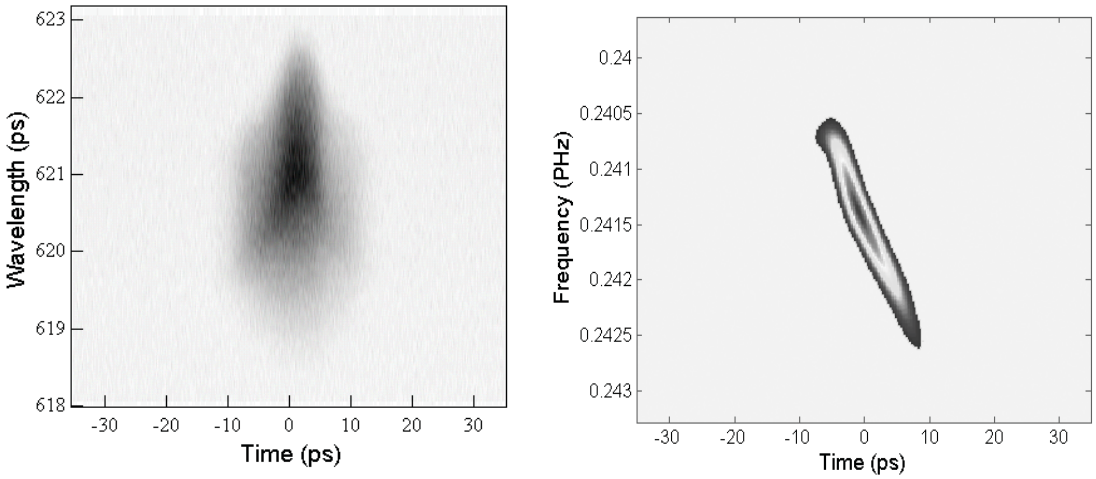

Fig. 9 (a) The SHG FROG trace from the 8-stack monolithic mode-locked QD laser with a gain current of 105mA and a reverse bias of 3.5V. (b) The spectrogram of the pulse retrieved from the SHG FROG trace shown in (a).

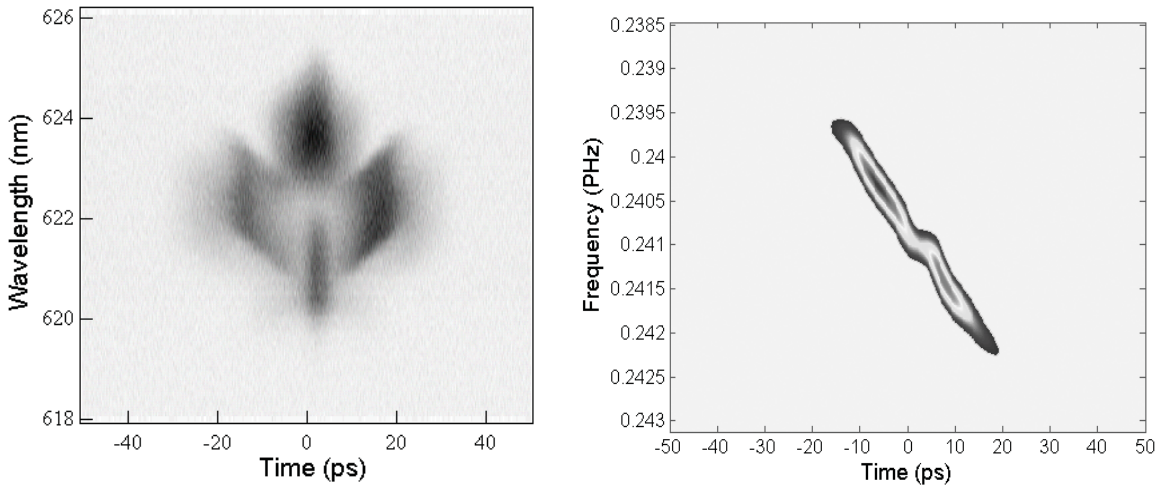

Fig. 10. (a) The SHG FROG trace from the 8-stack monolithic mode-locked QD laser with a gain current of 130mA and a reverse bias of 3.5V. (b) The spectrogram of the pulse retrieved from the SHG FROG trace shown in (a).

4. CONCLUSIONS

Quantum dot mode-locked lasers (QD MLLs) has sparked great interest since their first demonstration in 2001 as applications for optical time domain multiplexing, arbitrary waveform generation, two-photon sources, and optical clocking are anticipated. Ultrafast pulses from QD MLLs have been reported as short as 393 fs using intensity autocorrelation techniques, but detailed characterization examining the pulse shape, duration, chirp, and degree of coherence spiking in these lasers had been absent until recently. In this work, direct frequency-resolved optical gating (FROG) measurements on a QD MLL operating at a repetition rate of 5 GHz with typically 5-10 ps pulses have been

described. Since commercially available FROG devices lack the sensitivity required to measure the output pulses from QD MLLs, an ultra-sensitive second-harmonic-generation FROG system has been constructed. Good pulse retrievals were obtained from an 8.2-mm cavity length QD MLL that had a 1.1-mm long saturable absorber at average powers up to about 5-10 mW. FROG traces at higher average powers contained coherence spikes. These features are well known in intensity autocorrelations and are usually caused by laser instabilities, which are always "coherent" at zero time delay, causing a large and fictitiously narrow peak to occur. Unlike intensity autocorrelation, however, FROG is not susceptible to confusing these coherence spikes with the actual pulse width of the laser, and unambiguous measurement of the pulse shape and chirp can be obtained. The data showed a clear pulse asymmetry corresponding to a fast rise and slow fall time that has not been reported before. The mostly linear chirp in the pulses indicated that recompressing the output can produce sub-picosecond pulses.

5. REFERENCES

[i] Zhang, L., Cheng, L., Gray, A.L., Luong, S., Nagyvary, J., Nabulsi, F., Olona, L., Su, K., Tumolillo, T., Wang, R., Wiggins, C., Ziko, J., Zau, Z., Varangis, P.M., Su, H., and Lester, L. F., "5 GHz Optical Pulses From a Monolithic Two-Section Passively Mode-locked 1250/1310 nm Quantum Dot Laser for High Speed Optical Interconnects," Optical Fiber Communication Conference - Technical Digest - OFC/NFOEC OWM4 2005.

[ii] Gaburro, Z., "Optical interconnect," Silicon Photonics 94, 121-176 (2004).

[iii] Miller, D. A. B., "Rationale and challenges for optical interconnects to electronic chips," Proceedings of the IEEE 88(6), 728-749 (2000).

[iv] Keeler, G. A., Nelson, B. E., Agarwal, D., Debaes, C., Helman, N. C., Bhatnagar, A., and Miller, D. A. B., "The benefits of ultrashort optical pulses in optically interconnected systems," IEEE Journal of Selected Topics in Quantum Electronics 9(2), 477-485 (2003).

[v] Sotobayashi, H., Chujo, W., Konishi, A., and Ozeki, T., "Wavelength-band generation and transmission of 3.24-Tbit/s (81-channel WDMX40-Gbit/s) carrier-suppressed return-to-zero format by use of a single supercontinuum source for frequency standardization," Journal of the Optical Society of America B-Optical Physics 19(11), 2803-2809 (2002).

[vi] Mielke, M., Alphonse, G. A., and Delfyett, P. J., "168 channels x 6 GHz from a multiwavelength mode-locked semiconductor laser," IEEE Photonics Technology Letters 15(4), 501-503 (2003).

[vii] Bernstein, R., Chaffee, T. M., Diels, J. C., and Stahlkopf, K., "Apparatus and method for line of sight laser communication," United States Patent 09/215420, 1-6 (2002).

[viii] Arissian, L., and Dieals, J. C., "Mode-locked laser as a combined radio frequency and optical clock stabilized to a reference cavity, and calibrated through coherent interaction with rubidium," Proceeding of SPIE - Applications of Photonic Technology 5260, 1-10 (2003).

[ix] Diels, J. C., Arissian, L. "Applications of stabilized frequency combs to metrology," Proceedings of the SPIE - International Conference on Coherent and Nolinear Optics, and on Lasers, Applications and Technologies, (2005).

[x] Kolner, B. H. and Bloom, D. M., "Electrooptic Sampling In GaAs Integrated-Circuits," IEEE Journal Of Quantum Electronics 22(1), 79-93 (1986).

[xi] Williams, K. A., Thompson, M. G., and White, I. H., "Long-wavelength monolithic mode-locked diode lasers," New Journal of Physics 6(179), 1-30 (2004).

[xii] Xin, Y. C., Li, Y., Kovanis, V., Gray, A. L., Zhang, L., and Lester, L. F. "Reconfigurable quantum dot monolithic multi-section passive mode-locked lasers," Optics Express 15(22), 7623-7633 (2007).

[xiii] Rafailov, E. U., Cataluna, M. A., Sibbett, W., Il'inskaya, N. D., Zadiranov, Y. M., Zhukov, A. E., Ustinov, V. M., Livshits, D. A., Kovsh, A. R., and Ledentsov, N. N., "High-power picosecond and femtosecond pulse generation from a two-section mode-locked quantum-dot laser," Applied Physics Letters 87(8), 081107-1-081107-3 (2005).

[xiv] Xin, Y. C., Kane, D. J., and Lester, L. F., "Frequency-resolved optical gating characterisation of passively modelocked quantum-dot laser," Electronics Letters 44(21), 1255–1256 (2008).

[xv] N. G. Usechak, Y. C. Xin, C. Y. Lin, L. F. Lester, D. J. Kane, and V. Kovanis, "Modeling and Direct Electric-Field Measurements of Passively Mode-Locked Quantum-Dot Lasers," IEEE Journal of Selected Topics in Quantum Electronics 15(3), 653–660 (2009).

[xvi] G. Fiol, C. Meuer, H. Schmeckebier, D. Arsenijevic, S. Liebich, M. Laemmlin, M. Kuntz, and D. Bimberg, "Quantum-Dot Semiconductor Mode-Locked Lasers and Amplifiers at 40 GHz," IEEE Journal of Quantum Electronics 45(11), 1429–1435 (2009).

[xvii] Schmeckebier, H., Fiol, G., Meuer, C., Arsenijevic, D., and Bimberg, D., “Complete pulse characterization of quantum-dot mode-locked lasers suitable for optical communication up to 160 Gbit/s,” Optics Express 18(4), 3415-3425 (2010)

[xviii] Liu, G. T., Stintz, A., Li, H., Malloy, K. J., and Lester, L. F., "Extremely low room-temperature threshold current density diode lasers using InAs dots in In0.15Ga0.85As quantum well," Electronics Letters 35(14), 1163-1165 (1999).

[xix] Stintz, A., Liu, G. T., Gray, A. L., Spillers, R., Delgado, S. M., and Malloy, K. J., "Characterization of InAs quantum dots in strained InxGa1-xAs quantum wells," Journal of Vacuum Science & Technology B 18(3), 1496-1501 (2000).

[xx] Xin, Y. C., Li, Y., Martinez, A., Rotter, T. J., Su, H., Zhang, L., Gray, A. L., Luong, S., Sun, K., Zou, Z., Zilko, J., Varangis, P. M., and Lester, L. F., "Optical gain and absorption of quantum dots measured using an alternative segmented contact method," IEEE Journal of Quantum Electronics 42(7), 725-732 (2006).

[xxi] Huang, X. D., Stintz, A., Li, H., Lester, L. F., Cheng, J., and Malloy, K. J., "Passive mode-locking in 1.3 mu m two-section InAs quantum dot lasers," Applied Physics Letters 78(19), 2825-2827 (2001).

[xxii] Huang, X. D., Stintz, A., Li, H., Rice, A., Liu, G. T., Lester, L. F., Cheng, J., and Malloy, K. J., "Bistable operation of a two-section 1.3-mu m InAs quantum dot laser - Absorption saturation and the quantum confined Stark effect," IEEE Journal of Quantum Electronics 37(3), 414-417 (2001).

[xxiii] Sellin, R. L., Ribbat, C., Grundmann, M., Ledentsov, N. N., and Bimberg, D., "Close-to-ideal device characteristics of high-power InGaAs/GaAs quantum dot lasers," Applied Physics Letters 78(9), 1207-1209 (2001).

[xxiv] Kuntz, M., Fiol, G., Lammlin, M., Bimberg, D., Thompson, M. G., Tan, K. T., Marinelli, C., Penty, R. V., White, I. H., Ustinov, V. M., Zhukov, A. E., Shernyakov, Y. M., and Kovsh, A. R., "35 GHz mode-locking of 1.3um quantum dot lasers," Applied Physics Letters 85(5), 843-845 (2004).

[xxv] Kobrinsky, M. J., Block, B. A., Zheng, J. F., Barnett, B. C., Mohammed, E., Reshotko, M., Robertson, F., List, S., Young, I., and Cadien, C., "On-Chip Optical Interconnects,"Intel Technology Journal 8(2), 1-16 (2004).

[xxvi] Salib, M., Liao, L., Jones, R., Morse, M., Liu, A., Samara-Rubio, D., Alduino, D., and Paniccia, M., "Silicon Photonics," Intel Technology Journal 8(2), 143-161 (2004).